Molecular Systems Biology 8; Article number 623; doi:10.1038/msb.2012.55
Citation: ***Molecular Systems Biology*** **8:623**

www.molecularsystemsbiology.com

molecular systems biology

Regulation of yeast central metabolism by enzyme phosphorylation

Ana Paula Oliveira[1,3], Christina Ludwig[1,3], Paola Picotti[1], Maria Kogadeeva[1], Ruedi Aebersold[1,2] and Uwe Sauer[1,*]

[1] Department of Biology, Institute of Molecular Systems Biology, ETH Zurich, Zurich, Switzerland and [2] Faculty of Science, University of Zurich, Zurich, Switzerland
[3]These authors contributed equally to this work
* Corresponding author. Institute of Molecular Systems Biology, ETH Zurich, Wolfgang-Pauli-Str. 16, Zurich 8093, Switzerland. Tel.: +41 44 633 3672; Fax: +41 44 633 1051; E-mail: sauer@imsb.biol.ethz.ch

Received 7.5.12; accepted 5.10.12

As a frequent post-translational modification, protein phosphorylation regulates many cellular processes. Although several hundred phosphorylation sites have been mapped to metabolic enzymes in *Saccharomyces cerevisiae*, functionality was demonstrated for few of them. Here, we describe a novel approach to identify *in vivo* functionality of enzyme phosphorylation by combining flux analysis with proteomics and phosphoproteomics. Focusing on the network of 204 enzymes that constitute the yeast central carbon and amino-acid metabolism, we combined protein and phosphoprotein levels to identify 35 enzymes that change their degree of phosphorylation during growth under five conditions. Correlations between previously determined intracellular fluxes and phosphoprotein abundances provided first functional evidence for five novel phosphoregulated enzymes in this network, adding to nine known phosphoenzymes. For the pyruvate dehydrogenase complex E1 α subunit Pda1 and the newly identified phosphoregulated glycerol-3-phosphate dehydrogenase Gpd1 and phosphofructose-1-kinase complex β subunit Pfk2, we then validated functionality of specific phosphosites through absolute peptide quantification by targeted mass spectrometry, metabolomics and physiological flux analysis in mutants with genetically removed phosphosites. These results demonstrate the role of phosphorylation in controlling the metabolic flux realised by these three enzymes.
Molecular Systems Biology **8**:623; published online 13 November 2012; doi:10.1038/msb.2012.55
Subject Categories: proteomics; cellular metabolism
Keywords: metabolic flux; metabolism; phosphoproteome; post-translational regulation; selected reaction monitoring

Introduction

Microorganisms able to grow in a large spectrum of environmental conditions have evolved robust mechanisms to adjust the usage of carbon and nitrogen metabolic pathways according to their acute needs. Transcriptional regulation, arguably the best understood regulatory mechanism, has failed to explain many of the observed metabolic responses associated with these pathways. In the yeast *Saccharomyces cerevisiae*, for example, fluxes and kinetic activities of glycolytic enzymes are poorly explained by their transcript levels (Daran-Lapujade *et al*, 2004, 2007). These results suggest that post-transcriptional mechanisms are important to modulate the reaction rates and, in particular, post-translational phosphorylation is known to regulate activity of several enzymes in yeast central carbon and storage metabolism (Lin *et al*, 1996; Smith and Rutter, 2007; Oliveira and Sauer, 2012). Recent studies have revealed enzyme phosphorylation to be more widespread than previously appreciated, with about two-thirds of the *S. cerevisiae* metabolic proteins being targets of the kinase and phosphatase signalling network (Ptacek *et al*, 2005; Bodenmiller *et al*, 2010; Breitkreutz *et al*, 2010).

As a well-known post-translational modification, protein phosphorylation is involved in the regulation of many cellular processes, including metabolism (Krebs and Beavo, 1979), osmotic stress (Klipp *et al*, 2005), growth (Huber *et al*, 2009) and division (Tyson and Novak, 2008). In *S. cerevisiae*, reversible protein phosphorylation is regulated by about 120 kinases and 40 phosphatases (Bodenmiller *et al*, 2010). Phosphorylation can activate or inactivate a target protein by (i) altering its conformation; (ii) (un)blocking the access of a substrate to the catalytic centre; (iii) determining translocation between compartments; (iv) associating the protein to different protein complexes; or (v) marking the protein for degradation (Cohen, 2000; Serber and Ferrell, 2007). Generally, the functional role of protein phosphorylation is assessed by measuring its impact on activity, subcellular localisation or complex formation. Such functional assessement, however, is usually qualitative rather than quantitative owing to difficulties to accurately quantify protein phosphorylation and its effect on function.

Of the 681 enzymes and transporters constituting the *S. cerevisiae* genome-scale metabolic network considered here

(Costenoble *et al*, 2011), 237 have at least one phosphorylation site mapped in PhosphoPep, a repository of yeast phosphoproteome data (Bodenmiller *et al*, 2008). Functional relevance, however, has been demonstrated for only 17 of these metabolic proteins, nine of which are enzymes within the central carbon and amino-acid metabolism (Supplementary Table 1). These observations lead to two starting points for the here presented work. First, the discrepancy between the number of enzymes with detected and functionally verified phosphosites suggests that the majority of functional phosphoenyzmes are still unknown. Second, previous studies focused primarily on the qualitative effect of protein phosphorylation without considering the impact of phosphorylation on the operation of the metabolic network as whole.

Here, we investigate which enzyme phosphorylation events are important in regulating *S. cerevisiae* metabolism by focusing on the 204 enzymes that catalyse the 168 stoichiometrically distinct biochemical reactions of central carbon and amino-acid metabolism. For this purpose, we quantitatively measured the phosphoproteome of *S. cerevisiae* during growth under five environmental conditions using discovery-driven mass spectrometry (MS), and combined these data with previously determined protein abundances and flux estimates (Costenoble *et al*, 2011). For the 35 differentially phosphorylated enzymes, we investigated the effect of these regulatory events in the context of the whole metabolic network operation, by correlating intracellular metabolic fluxes with relative measurements of total or phosphorylated protein abundances across conditions. Where the non-phosphorylated protein appeared to be the active enzyme, we quantified absolute phosphorylated and non-phosphorylated protein abundances directly from the crude cell extract by selected reaction monitoring (SRM). The functional *in vivo* impact of selected enzyme phosphosites was evaluated through physiological and metabolic characterisation of phosphorylation-deficient mutants. Through the here established approach to quantitatively relate phosphorylation status with physiological enzyme activity, we identified five new enzymes that are regulated by post-translational phosphorylation and provided functional insights for two of them.

Results

Quantitative phosphopeptide patterns under five nutritional conditions

To identify phosphorylation sites that regulate metabolic enzymes, we isolated phosphopeptides from yeast cells during steady-state growth under five nutritional conditions and generated quantitative phosphopeptide patterns from each isolate, using liquid chromatography tandem MS (LC-MS/MS). The conditions were four minimal media cultures grown either aerobically in glucose, galactose or ethanol, or anaerobically in glucose, and one complex media culture grown in yeast-extract/peptone. These conditions were chosen to cover different modes of metabolic operation—from glycolysis to gluconeogenesis, from fermentative and respiro-fermentative to fully respiratory—and hence are pertinent for a functional analysis that relates phosphorylation changes to differential metabolic activity. Culture samples for phosphoproteome analysis were taken at pseudo steady state during the mid-exponential growth phase. The entire cellular protein contents were extracted, the crude cell extracts trypsinised and the resulting peptides were enriched for phosphopeptides by TiO_2 chromatography (Larsen *et al*, 2005; Bodenmiller and Aebersold, 2010) (Figure 1A). The phosphopeptide mixtures from three independent biological replicates were analysed twice each by label-free, quantitative shotgun proteomics using high-resolution MS. The resulting MS data were processed for peptide identification and quantification as described in the Supplementary Materials and Methods. Fold-changes in phosphopeptide abundance were calculated as the average peak intensity upon growth in each nutrient condition relative to the average peak intensity for glucose-grown samples.

Without using extensive phosphopeptide sample fractionation, across all conditions we identified 556 proteins with at least one phosphorylation site, from a total of 1300 phosphopeptides matching to 1265 unique phosphorylation sites (Supplementary Table 2). This corresponds to about 13% of the proteins typically expressed in yeast cells (de Godoy *et al*, 2008). The phosphoproteins were generally annotated to be involved in RNA and DNA metabolism, transcription, cell cycle and response to stress. Gene ontology analysis further revealed an over-representation of proteins involved in carbohydrate and nitrogen metabolism (SGD TermFinder; $P<0.05$), suggesting that protein phosphorylation plays an important role in metabolic regulation.

Of the 681 enzymes contained in the reaction network of yeast metabolism (Costenoble *et al*, 2011), we identified 70 with at least one phosphorylation site in at least one of the five conditions (Supplementary Table 2), 10 of which do not have a phosphorylation site yet listed in PhosphoPep. For 61 of the 70 phosphoenzymes, phosphorylation fold-changes were greater than two-fold in at least one condition relative to glucose and the phosphorylation patterns were condition dependent (Supplementary Figure 1), indicating frequent occurrence of post-translational phosphorylation in yeast metabolism. The 70 phosphorylatable enzymes distribute across a variety of metabolic pathways, including essentially all of central carbon, carbohydrate storage, amino-acid, lipid, nucleotide, cofactor and phosphate metabolism. Most of these enzymes catalyse irreversible reactions. In that category, they are significantly over-represented relative to the entire network (hypergeometric test; $P<0.05$). Because some metabolic reactions involve the transfer of a phosphate group to metabolites, we investigated whether the observed phosphorylation was due to self-phosphorylation at the catalytic centre. Since only 25 of the 70 phosphoenzymes catalysed the transfer of phosphate groups and none of the identified phosphosites coincided with known or predicted ATP-binding sites and/or catalytic centres of phosphate-transfer enzymes, we ruled out such self-phosphorylation.

Combining proteome and phosphoproteome data to quantify the degree of phosphorylation

The degree to which a protein is phosphorylated, that is, the fraction of phosphosite occupancy, has been suggested as a

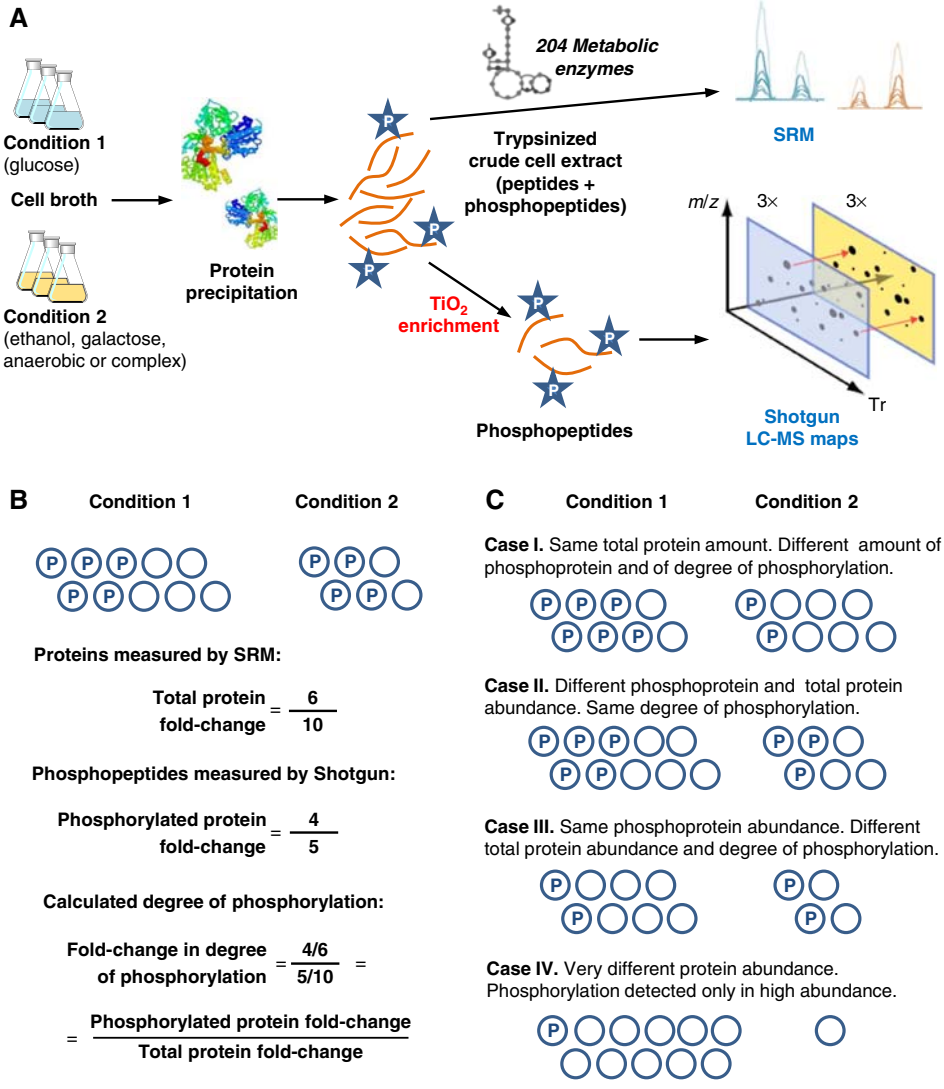

Figure 1 Workflow to determine changes in protein, phosphoprotein and degree of phosphorylation of metabolic enzymes. (**A**) Wild-type *S. cerevisiae* was cultivated under five different nutritional conditions in biological triplicates. Cells were harvested at mid-exponential phase and lysed, followed by protein precipitation and digestion with trypsin. An aliquot of trypsinised crude cell extract was phosphoenriched and phosphopeptides were analysed by shotgun. Another aliquot was used for relative quantification of total protein for 204 pre-selected metabolic enzymes by SRM (Costenoble *et al*, 2011). (**B**) Schematic representation of the abundance fold-change measured (total protein and phosphoprotein fold-change) and derived (degree of phosphorylation fold-change) in this study. (**C**) Four scenarios of how total protein and phosphoprotein changes relate.

more accurate way to assess the functional significance of regulation by phosphorylation (Olsen *et al*, 2010; Wu *et al*, 2011a). Here, we focus on the 204 enzymes that catalyse the 168 stoichiometrically distinct biochemical reactions covering essentially all central carbon and amino-acid metabolism. Based on the previously quantified protein abundances of these 204 enzymes under the same five conditions used here (Costenoble *et al*, 2011), we combined the proteome and phosphoproteome measurements to determine changes in the degree of phosphorylation across all five conditions. Protein abundances were quantified in a targeted MS approach based on SRM (Picotti *et al*, 2009), from the same crude cell extracts used here for phosphoproteome analysis (Figure 1A). We determined fold-changes in the degree of phosphorylation by dividing the phosphoprotein abundance fold-change by the protein fold-change, all relative to the glucose condition (Figure 1B). Of the 70 here detected phosphoenzymes, 35 were members of the 204 enzymes network, all of which changed the degree of phosphorylation and/or the phosphoprotein abundance by more than two-fold in at least one condition relative to glucose (Supplementary Table 2). These differentially phosphorylated enzymes are concentrated in the upper glycolysis, around the pyruvate branch point and in carbohydrate storage pathways (Figure 2).

Combining total protein and phosphoprotein changes allowed us to discriminate four different scenarios (Figure 1C; Supplementary Table 2). In case I, the amount of phosphoprotein changes but not the total protein abundance. This was observed for 20 enzymes in at least one condition, with phosphoforms of Gsy2, Pfk2 and Tsl1 falling within this

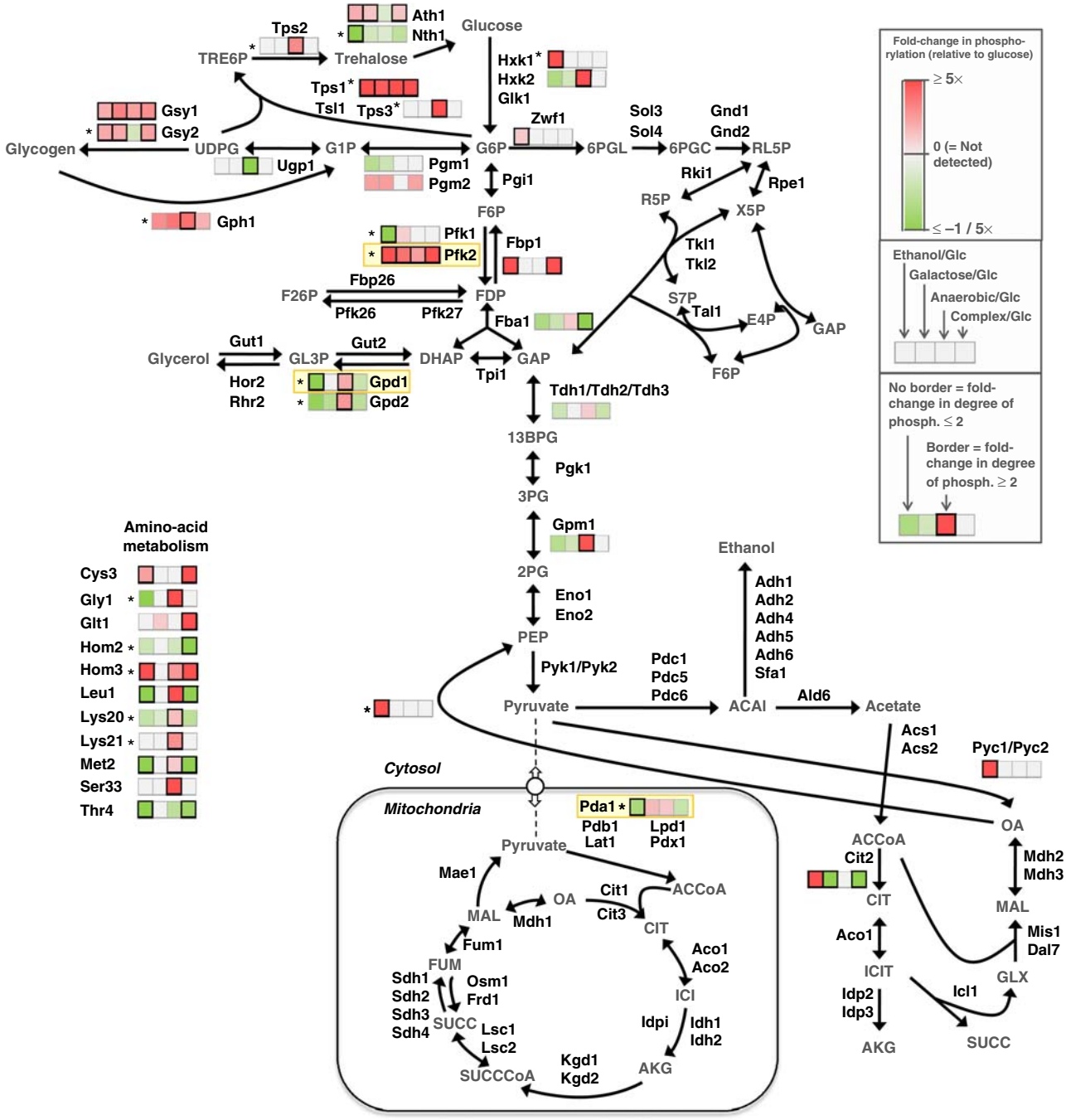

Figure 2 Phosphoenzyme fold-changes mapped onto the yeast central carbon and amino-acid metabolic network. The 35 phosphoenyzmes unambiguously quantified are shown. In addition, we detected but could not resolve the phosphoforms of Pyc1/Pyc2 and Tdh1/Tdh2/Tdh3, because their phosphopeptides were shared by all isoenzyme species (Supplementary Table 2). Positive (/negative) fold-changes indicate higher occurrence in ethanol, galactose, anaerobic or YP condition (/glucose). Change in degree of phosphorylation by more than two-fold is marked with a thick border. Proteins marked with an asterisk have phosphosites quantified by more than one phosphopeptide. Yellow boxes highlight the three enzymes that we followed-up.

scenario in three or more conditions. In case II, both protein and phosphorylated protein change proportionally, resulting in no change in degree of phosphorylation, a case discarded when assessing functionality based solely on the degree of phosphorylation. We found nine enzymes within this category: Fba1, Gly1, Gpd2, Gph1, Lys20, Nth1, Pgm1 and Pgm2. In case III, the total amount of protein changes but not the phosphorylated protein (or it changes in the opposite direction). We found eight enzymes in this category: Ath1, Gph1, Leu1, Lys20, Lys21, Met2, Pfk2 and Zwf1. For Pfk2 (also in case I), Gph1 and Lys20 (also in case II), changes occurred in different phosphoforms. While case I clearly represents

differential post-translational phosphorylation, cases II and III imply regulation either by post-translational phosphorylation or by total protein degradation/synthesis. Lastly, in case IV, the total protein changes extensively but phosphorylation is only detected in the high-abundance condition. We found Fbp1 and Pck1, two gluconeogenic enzymes, within this category. Since for Fbp1 phosphorylation was reported to be a signal for degradation (Holzer and Purwin, 1986), our protein and phosphorylation data on Pck1 suggests, by analogy, that phosphorylation is also a signal for Pck1 degradation. This hypothesis is further supported by the location of the phosphosite within 15 amino acids from the N-terminus.

Globally, about 75% of the phosphorylation changes varied by more than two-fold both at the level of phosphoprotein abundance and phosphorylation degree, a percentage in accordance with previous studies (Wu *et al*, 2011a). To obtain evidence whether these phosphorylation changes actually represent functional regulatory events, in the following we specifically address the question of whether phosphorylation activates or inhibits an enzyme and what the functional impact of this modulation would be on metabolic operation.

Phosphorylation as a mechanism to modulate the pool of catalytically competent enzyme

Among the 204 enzymes of central carbon and amino-acid metabolism quantified by targeted proteomics, the impact of phosphorylation on enzyme activity has been known for nine enzymes (Supplementary Table 1), seven of which we found to be phosphorylated in this study. Of the nine cases, published *in vitro* enzyme activity data showed that phosphorylation activates Gph1, Hxk2, Nth1 and Pyk1 (/Cdc19), inhibits Fbp1, Gdh2, Gsy2 and Pda1, and regulates the reaction location for Ugp1 (Supplementary Table 1). In all cases except Gdh2, the functional phosphosites have been identified. The literature data generally fits our observed conditions of higher phosphorylation. For example, the higher activity of the neutral trehalase Nth1 in glucose was shown to be associated with high phosphorylation of several phosphosites (Wera *et al*, 1999), while lower activity in ethanol is associated with very low phosphorylation (San Miguel and Arguelles, 1994; Wera *et al*, 1999). Accordingly, we found in our study the three phosphosites T58, S60 and S83 phosphorylated in glucose but not in ethanol (Supplementary Table 2). The activity of the pyruvate dehydrogenase complex E1 α subunit Pda1 was shown to be inactivated by phosphorylation at site S313 (Uhlinger *et al*, 1986; Krause-Buchholz *et al*, 2006), and activity is higher in ethanol than in glucose (Wenzel *et al*, 1993). Accordingly, we observed higher phosphorylation in glucose than in ethanol.

Besides the observations in yeast and other organisms that enzyme phosphorylation impacts mostly catalytic activity by either activation or inhibition, several studies have also shown that the degree of phosphorylation is not binary (Huttlin *et al*, 2010; Wu *et al*, 2011a, b) and can undergo vast changes across cellular stages (Olsen *et al*, 2010). Together, these observations point towards a model of phosphorylation as a mechanism that modulates the pool of catalytically competent enzyme. The catalytically competent enzyme could be either the phosphorylated or the non-phosphorylated form, such that phosphorylation activates or inhibits activity, respectively (Figure 3A). For enzymes that are not post-translationally modified, the activity will instead be determined by the total protein abundance (Figure 3A). Given the availability of measurements for reaction rates, total protein, phosphoprotein and non-phosphoprotein, the dependency between reaction rate and the catalytically competent pool is therefore expected to be better than with the other protein pools (Figure 3B). Such a model is valid if the reaction rate is determined by the amount of active enzyme rather than by the concentration of the limiting substrate and if no other allosteric or post-translational modification occurs (Gerosa and Sauer, 2011; Oliveira and Sauer, 2012). In the case of isoenzymes, it may be difficult to assess which species catalyses the reaction in a particular condition, hindering the dependency between the reaction rate and the catalytic competent pool.

Functional relevance of enzyme phosphorylation in the context of the whole metabolic system

Metabolic fluxes, that is, *in vivo* reaction rates, reflect the integrated response of all levels of cellular regulation (Sauer, 2006). To investigate the relevance of phosphorylation in regulating enzyme functioning at physiological levels, we related phosphorylation changes with metabolic fluxes that were previously quantified under our conditions and for all reactions constituting the metabolic network (Costenoble *et al*, 2011). Specifically, we calculated the Pearson correlation coefficient between fluxes and the relative measurements of total protein or phosphorylated protein abundances of the enzymes realising those fluxes, across the four well-defined conditions aerobic glucose, ethanol and galactose, and anaerobic glucose (Supplementary Figure 2). We considered absolute flux values, ignored enzymes with a reaction flux of zero in at least two conditions and selected phosphoproteins that were quantified in at least three conditions. This resulted in correlations for 16 phosphopeptides, corresponding to 11 enzymes, of which Gpd1 and Pfk2 occurred in multiple phosphorylated forms. The remaining phosphoenzymes could not be analysed due to lack of data to sustain correlations. We note that relative amounts of total and phosphorylated protein are suitable for the correlation analysis because they are proportional by a scalar to the absolute levels, though they do not directly allow the estimation of changes in the non-phosphorylated protein (Supplementary Figure 3).

To identify candidate enzymes that could be regulated by phosphorylation, we assessed the statistical significance of each correlation coefficient and selected those that showed either a good positive or negative correlation ($P<0.10$) between flux and phosphorylated protein. In particular, significant positive correlations were found for Fba1[S313^{P}], Gpd1[S25^{P}] and Gpd2[S72^{P}, S75^{P}], suggesting that the phosphoprotein would be the catalytically competent form in these cases (Figure 3C). For Gpd1 and Gpd2 we cannot differentiate the role of phosphorylation between them because they are isoenzymes with glycerol-3-phosphate dehydrogenase activity and therefore the flux values reflect the sum of both isoenzymes to the reaction rate. Negative

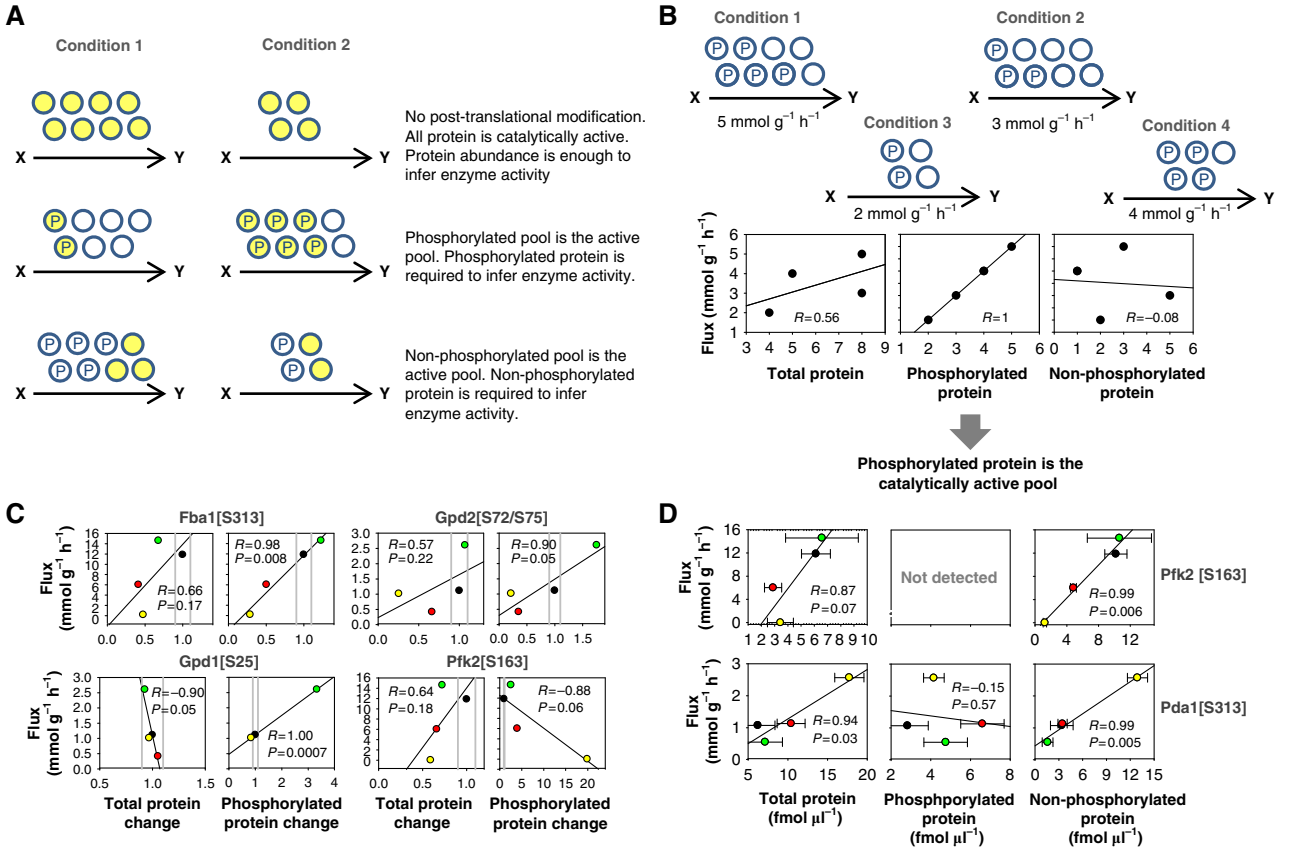

Figure 3 Correlation analysis between flux and total protein or phosphoprotein abundances. (**A**) Schematic representation of phosphorylation being a mechanism to determine the pool of catalytically competent enzyme (in yellow). (**B**) Schematic example of how to identify the pool of catalytically competent enzyme given measurements of enzyme activity, total protein, phosphoprotein, and non-phosphoprotein. If the catalytically competent enzyme is the non-phosphoprotein, a good correlation would be instead found between flux and non-phosphorylated protein pool. (**C**) Correlation coefficients (R) between flux and total or phosphoprotein abundance fold-changes determined by shotgun phosphoproteomics for enzymes with significant correlation ($P<0.10$) between flux and phosphorylated protein. The four points correspond to glucose (black), galactose (red), anaerobic (green) and ethanol (yellow). Glucose is always the unit reference point. Vertical bars mark 10% more or less (phospho)protein relative to the glucose condition. (**D**) Correlations between flux and absolute concentrations of total, phospho and non-phosphoprotein determined directly from crude cell extracts for Pfk2 at site S163 and Pda1 at site S313 using SRM. Conditions and colour scheme are the same as described in (C).

correlations were found for Pda1[S313^{P}] and Pfk2[S163^{P}], suggesting that here phosphorylation inhibits activity (Figure 3C; Supplementary Figure 2). Weaker positive correlations ($P<0.20$) were found for Gpd1[S24^{P}, S27^{P}], Gpm1[S116^{P}], Lys20[T396^{P}], Pfk1[S179^{P}] and Pfk2[S171^{P}], while for Pgm1, Pgm2 and Thr4 correlations were too weak to assign a trend.

Overall, our more stringent significance criteria provide evidence for not previously known phosphoregulation that modulates the system level activity of four enzymes—Fba1, Gpd1, Gpd2 and Pfk2—, adding to our previously hypothesised role of phosphorylation as a signal for Pck1 degradation. For the multiple phosphorylation sites in Gpd1, Gpd2 and Pfk2, we verified the positions of phosphorylation through SRM measurements of the phosphoenriched, glucose-grown samples by comparing the sample traces against isotopically labelled synthetic reference phosphopeptides (Supplementary Figure 4). We thereby confirmed the phosphorylation sites S24 and S27 of Gpd1, S72 and S75 of Gpd2 and S163 of Pfk2. Since Pfk2, the β subunit of the phosphofructose-1-kinase complex, and Gpd1, a glycerol-3-phosphate dehydrogenase, are key enzymes in glycolysis and stress response, respectively (Figure 2), we used in the following two molecular approaches to validate the functional role of their phosphorylation; that is, specific phosphosite quantification and functional evaluation of the genetic removal of phosphosites.

Determination of non-phosphorylated protein is required for accurate verification when phosphorylation inhibits enzyme activity

One limitation of correlating flux and phosphorylation levels occurs when the non-phosphorylated form is the catalytically competent enzyme and the total protein abundance varies, as illustrated in the Supplementary Figure 3. This is particularly a problem when fold-changes for total protein and phosphoprotein are available instead of absolute amounts, since the fold-change of the non-phosphoprotein cannot be derived from them. To address this limitation and to confidently assess the

role of S163 phosphorylation on Pfk2 activity, we applied a phosphoproteomics approach to quantify absolute concentrations of total, phosphorylated and non-phosphorylated protein directly from the trypsinised crude cell extract using a targeted MS method based on SRM. We applied the approach to Pda1 and Pfk2, two enzymes whose activity is known (Pda1) or here hypothesised (Pfk2) to be inhibited by phosphorylation at sites S313 and S163, respectively. Using isotope-labelled and calibrated reference peptides, we determined total, phosphorylated and non-phosphorylated protein for wild-type yeast grown under the four well-defined conditions described earlier in this study (Supplementary Table 2; Supplementary Figures 5 and 6). For Pda1, we observed that the sum of phospho- and corresponding non-phosphopeptide was always comparable to the total amount of protein determined independently, highlighting the high quality and accuracy of the measurement. In case of Pfk2, the phosphopeptide could not be detected in the crude cell extract, although it could be detected in the phosphoenriched samples (Supplementary Figure 4), which may be attributed to low peptide concentration, low MS-response factor or to the occurrence of alternative peptide forms. However, we observed that the non-phosphopeptide was abundant in glucose and scarce in ethanol, suggesting that the major portion of this Pfk2 peptide is modified in ethanol. For both Pda1 and Pfk2, the very good correlation between flux and the non-phosphorylated protein (Figure 3D) strongly supports our expectation that the catalytically competent enzyme is the non-phosphorylated form, that is, phosphorylation inhibits activity. The determined absolute concentrations also allowed us to calculate the absolute degree of phosphorylation for Pda1, which varied between 20% (±10%) in ethanol and 70% (±8%) under anaerobic condition.

Identification of functional phosphorylation sites for Pfk2 and Gpd1

To assign functional relevance to specific phosphosites and to quantify individual contributions of multiple phosphosites to enzyme function, we replaced phosphorylated serine residues by non-phosphorylatable alanine through site-directed mutagenesis of S163, S167 and S171 of Pfk2, S23, S24, S25 and S27 of Gpd1 and, as positive control, S313 of Pda1 (Figure 4A). The *in vivo* impact of phosphosite removal on metabolism was evaluated by (i) following growth in the previously identified high-phosphorylation condition and analysing how growth physiology was affected and (ii) determining the intracellular concentration of substrate and product metabolites in the different phosphosite mutants during growth in the high-phosphorylation condition.

The phosphosite S313 of Pda1 is a well-reported functional site modulating the *in vitro* activity of this subunit of the pyruvate dehydrogenase complex (Uhlinger *et al*, 1986; Krause-Buchholz *et al*, 2006; Gey *et al*, 2008), though the *in vivo* consequences of such phosphorylation have never been demonstrated. Consistent with the known *in vitro* inhibitory role of phosphorylation at site S313, the phosphorylation-deficient mutant Pda1[S313A] exhibited increased pyruvate dehydrogenase flux and further on through part of tricarboxylic acid (TCA) cycle to α-ketoglutarate during growth on glucose (Figure 4B; Supplementary Table 3). This flux increase is apparent from the increased extracellular yields of α-ketoglutarate and glutamine at unchanged biomass yields. The overflow to α-ketoglutarate and glutamine rather than a complete cyclic flux through the TCA cycle occurs probably because the remaining portion of the TCA cycle and the respiratory chain remain transcriptionally repressed on glucose (Gancedo, 1998; Westergaard *et al*, 2007; Fendt *et al*, 2010). To cope with increased NADH production that results from the higher pyruvate dehydrogenase flux, the phosphorylation-deficient mutant also displayed increased glycerol yield to reoxidise NADH (Figure 4B).

Of the three individually tested Pfk2 sites S163, S167 and S171, only the Pfk2[S163A] mutant exhibited a growth phenotype on gluconeogenic carbon sources, namely a 20% lower biomass yield on ethanol than the reference strain (Figure 4C; Supplementary Table 3). To confirm causality of altered Pfk2 activity on the altered physiology, we determined intracellular concentrations of the reaction substrate and product for all Pfk2 mutants and reference strain during growth in ethanol (Figure 4C; Supplementary Table 3). As expected from the silent phenotype of the Pfk2[S167A] and Pfk2[S171A] mutants, their intracellular concentrations were indistinguishable from the reference strain. Consistent with the hypothesis that phosphorylation inhibits phosphofructose-1-kinase activity, the concentration of the reaction product fructose 1,6-bisphosphate was two-fold higher in the Pfk2[S163A] mutant, while a Δ*pfk2* deletion mutant exhibited the opposite response with three-fold lower fructose 1,6-bisphosphate concentrations. Increased levels of fructose 1,6-bisphosphate in the Pfk2[S163A] mutant, which is now permanently active under the gluconeogenic conditions when its activity is not required, suggest a futile cycle activity at the PFK/FBPase node. Further evidence for the occurence of such an ATP-dissipating futile cycle in the Pfk2[S163A] mutant comes from the about 20% reduced biomass yield.

Finally, we evaluated the impact of individual and combined phosphosite loss in Gpd1, the key glycerol-3-phosphate dehydrogenase involved in osmo-regulation (Ansell *et al*, 1997) and the only isoenzyme affecting the glycerol yield during aerobic growth in glucose (Supplementary Table 3). Since none of the single point mutants, Gpd1[S23A], Gpd1[S24A], Gpd1[S25A] and Gpd1[S27A], exhibited altered growth rates on glucose (Supplementary Table 3), we constructed also the double Gpd1[S24/27A], the triple Gpd1[S23/24/25A] and the quadruple Gpd1[S23/24/25/27A] point mutants. Only the mutant lacking all four sites exhibited a physiological phenotype, with two-fold higher glycerol yield relative to the reference strain (Figure 4D; Supplementary Table 3). Further corroborating that all four sites are required for enzyme regulation by phosphorylation, only the quadruple point mutant showed higher *in vitro* glycerol-3-phosphate dehydrogenase activity (Figure 4D). Consistent with the higher *in vitro* activity of the Gpd1[S23/24/25/27A] mutant, the intracellular concentration of the reaction product glycerol-3-phosphate were two-fold higher in the quadruple point mutant and five times lower in the *Δgpd1* knockout, while in the other mutants the levels remained

A

Enzyme	Phosphopeptide	Phosphosite	Fold-change (Eth/Glc)	Constructed site mutations
Gpd1 (YDL022W)	RSS[P]SSVS[P]LK	S23,S27	–6.2	Gpd1[S23A] Gpd1[S24A] Gpd1[S25A] Gpd1[S27A] Gpd1[S24/27A] Gpd1[S23/24/25A] Gpd1[S23/24/25/27A]
	SSS[P]SVS[P]LK	S24,S27	–2.0	
	SSS[P]SVS[P]LKAAEKPFK	S24,S27	–6.2	
	SSS[P]SVSLK	S24	–3.3	
	SSSS[P]VSLK	S25	–1.2	
Pda1 (YER178W)	YGGHS[P]MSDPGTTYR	S313	–3.6	Pda1[S313A]
Pfk2 (YMR205C)	NAVSTKPTPPPAPEASAES[P]GLSSK	S163	19.9	Pfk2[S163A] Pfk2[S167A] Pfk2[S171A]
	NAVSTKPTPPPAPEASAESGLSS[P]KVHS[P]YTDLAYR	S167,S171	1.8	
	NAVSTKPTPPPAPEASAES[P]GLSS[P]KVHS[P]YTDLAYR	S163,S167,S171	Only ethanol	

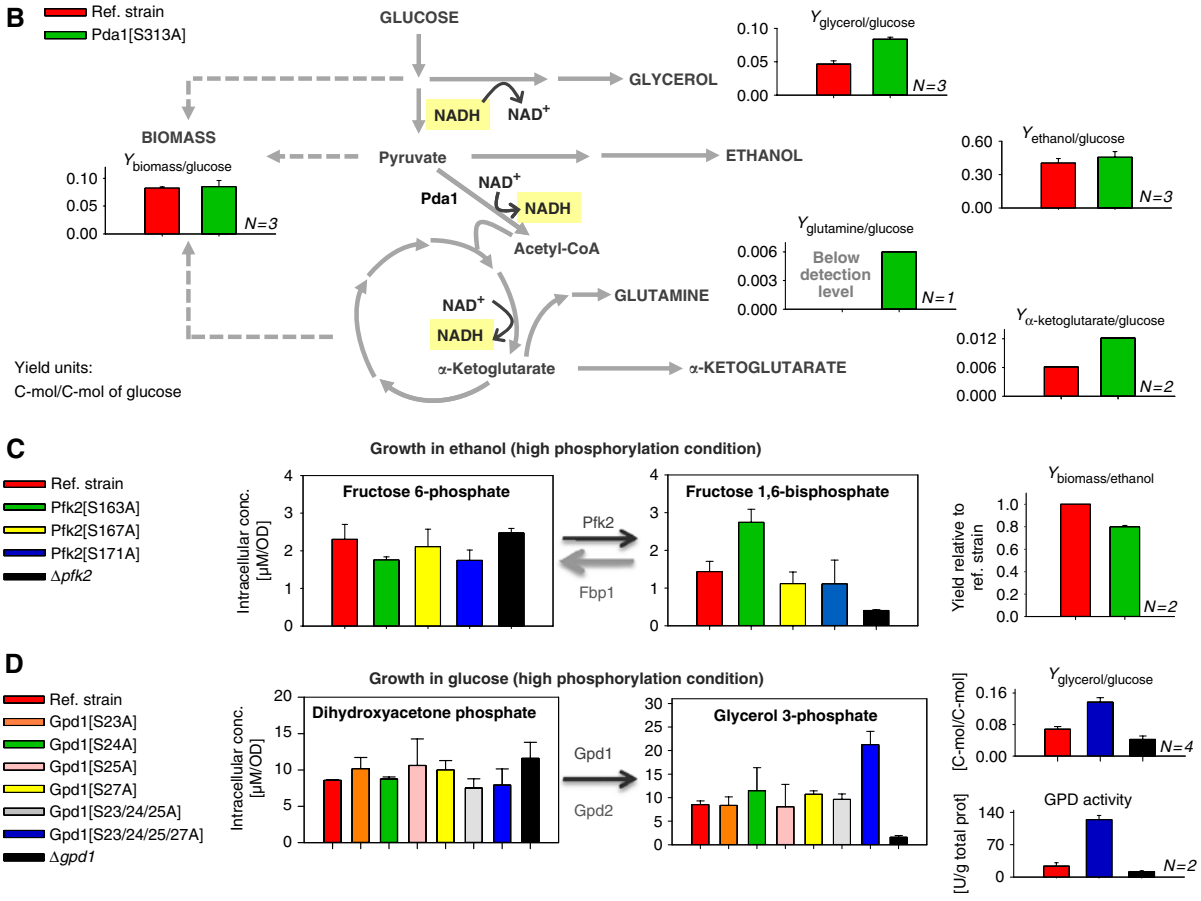

Figure 4 Functional impact of phosphosite removal on metabolic activity. (**A**) List of followed up proteins and phosphosites. All relevant phosphopeptides detected by shotgun phosphoproteomics are listed, as well as the corresponding phosphorylation sites and the fold-changes between ethanol and glucose, with a negative value indicating higher abundance in glucose. Phosphosite-deficient mutants were constructed through site-directed mutagenesis by replacing serine by alanine. (**B**) Evidence for increased pyruvate dehydrogenase activity in the Pda1[S313A] mutant. Relative to the reference strain, the point mutant displayed increased secretion of α-ketoglutarate, glutamine and glycerol during growth in glucose. Extracellular compounds are written in uppercase. (**C**) Impact of Pfk2 phosphosite loss on the *in vivo* enzyme activity during growth in ethanol. Only the mutant Pfk2[S163A] displayed different intracellular metabolite levels of reaction product and 20% decreased biomass. Due to the difficulty to control ethanol evaporation, the biomass yield on ethanol is given as relative measurements for strains grown and measured on the same day. (**D**) Impact of Gpd1 phosphosite loss on the *in vivo* and *in vitro* enzyme activity during growth in glucose. Only the quadruple point mutant Gpd1[S23/24/25/27A] displayed different intracellular metabolite levels of reaction product, increased glycerol yield and increased glycerol-3-phosphate dehydrogenase activity.

unchanged relative to the reference strain (Figure 4D). These results unambiguously show that loss of all four phosphosites increases Gpd1 activity, indicating that phosphorylation inhibits Gpd1.

Discussion

Reversible phosphorylation is a common post-translational modification to regulate protein function. The extent and

relevance of phosphoregulation for metabolic enzymes in yeast, however, has been limited to *in vitro* studies on few particular enzymes, mostly carried out before the 1990s (Oliveira and Sauer, 2012). Here, we developed a novel approach to assess functional consequences of phosphorylation events in the context of the entire *in vivo* operation of the metabolic network, driving testable hypotheses on enzyme activity inhibition or activation. From the 35 enzymes in *S. cerevisiae* central carbon and amino-acid metabolism that were differentially phosphorylated in at least one of the five tested nutritional conditions, we assessed potential phosphoregulation through the correlation of phosphoprotein abundances with metabolic fluxes, for the subset of enzymes where fluxes where available. These intracellular fluxes are better representatives of the *in vivo* enzyme functioning than *in vitro* determined enzyme activities, since they reflect the integrated response of the metabolic and regulatory system (Sauer, 2006). Five previously unknown functional phosphoenzyme candidates were thereby identified within central metabolism, and two were validated through experimental follow-ups.

Functional interpretation of phosphorylation observed in phosphoproteome studies often relies on abundance changes of phosphoproteins. Following the notion that function is better assessed by normalising the phosphoprotein form to the total protein (i.e., the degree of phosphorylation) (Wu *et al*, 2009, 2011a; Huttlin *et al*, 2010; Olsen *et al*, 2010), we quantified changes in the degree of phosphorylation for the 35 enzymes by combining phosphopeptide with total protein changes determined by shotgun phosphoproteomics and SRM, respectively. Primarily in upper glycolysis, around the pyruvate node and in carbohydrate storage pathways, many enzymes underwent vast fold-changes in the degree of phosphorylation across conditions, which can reflect changes at different levels of phosphorylation occupancy. For Pda1, we verified that the absolute fraction of phosphorylation occupancy varied between 20% in ethanol and 70% in anaerobic glucose, revealing that in this case phosphorylation affects a large fraction of the enzyme. Furthermore, functionality of Pda1, assessed in terms of metabolic flux, correlated better with the absolute amount of non-phosphoprotein than with the degree of phosphorylation, suggesting that the degree of phosphorylation may be misleading for functional interpretation of phosphorylation, in particular when phosphorylation inhibits enzyme activity.

While changes in phosphoprotein abundance imply a differential regulatory activity by protein kinases and/or phosphatases, the functional consequence of this phosphorylation on enzyme activity and metabolic fluxes is less obvious. In fact, evolutionary studies suggested that 65% of all phosphorylation sites are non-functional (Landry *et al*, 2009) and recently it was shown that metabolite-binding allostery, but not phosphorylation, plays a predominant role in regulating the metabolic flux through the pyruvate kinase Pyk1 (/Cdc19) (Xu *et al*, 2012). Here, we assessed functionality of particular phosphosites by analysing how the corresponding phosphopeptide abundance correlated with metabolic flux. Based on the hypothesis that phosphorylation modulates the pool of catalytic competent enzyme, our correlation analysis allowed us to infer the role of phosphorylation for five enzymes, Pda1, Fba1, Gpd1, Gpd2 and Pfk2, the latter four of which were previously not known to be phosphoregulated. For six other enzymes, correlations were either not significant or too weak to assign a trend, which may be due to inaccurate flux or phosphorylation abundance estimations, the occurrence of allosteric or other post-translational regulation events, or a non-functional phosphorylation. We did not apply the correlation analysis to phosphopeptides that were detected in less than three conditions and to storage carbohydrate pathways, for which fluxes could not be estimated using flux balance analysis. In addition to the four new cases of enzyme regulation by phosphorylation inferred above, we further hypothesised that, by analogy with the reported Fbp1 case (Holzer and Purwin, 1986), the also gluconeogenic enzyme Pck1 is likely flagged for protein degradation through phosphorylation at its N-terminus. These five newly described candidate cases expand the number of previously known phosphoregulated enzymes in yeast central carbon and amino-acid metabolism by >50%. For the remaining 23 phosphoenzymes, the present data are insufficient to conclude on the functional relevance of their phosphosites.

To validate the functional impact of some of the hypothesised phosphorylation sites and to demonstrate their causality in controlling fluxes, we removed specific phosphosites of Pda1, Pfk2 and Gpd1. Phosphorylation of S313 of Pda1 is well known to inhibit the *in vitro* activity of the pyruvate dehydrogenase complex (Uhlinger *et al*, 1986; Krause-Buchholz *et al*, 2006; Gey *et al*, 2008), but the *in vivo* consequences of the phosphorylation have not been demonstrated. Through quantitative physiology in the phosphorylation-deficient mutant Pda1[S313A], we demonstrated here that this phosphorylation event indeed controls the *in vivo* flux through pyruvate dehydrogenase complex during growth on glucose.

For Pfk2 we found that phosphosite S163, but not S167 and S171, inhibit *in vivo* phosphofructokinase activity. This was corroborated by three observations: (i) the absolute amount of the non-phosphorylated peptide (representing the active enzyme) at site S163 showed a very good positive correlation with the flux through the phosphofructokinase reaction; (ii) the Pfk2[S163A] mutant, which is resilient to inhibition, had increased levels of the reaction product under ethanol growth conditions when the reaction is supposed to be inactive, while the complete deletion *Δpfk2* displayed the opposite behavior with lower intracellular reaction product levels; and (iii) the Pfk2[S163A] mutant displayed 20% reduced biomass yield on ethanol relative to the reference strain. The latter suggests the operation of an ATP-dissipating futile cycle at the PFK/FBPase node in the phosphorylation-deficient mutant during growth in gluconeogenic conditions. Conjointly with Pfk1, Pfk2 catalyses the formation of fructose 1,6-bisphosphate from fructose 6-phosphate as the α and β subunits of the 6-phosphofructo-1-kinase complex, respectively. In many eukaryotes, including mammals, 6-phosphofructose-1-kinase is regulated by post-translational phosphorylation (Kemp and Foe, 1983; Legisa and Bencina, 1994; Fernandez *et al*, 1997). A single yeast report describes phosphorylated Pfk2 upon incubation with radioactive-labelled ATP, with phosphorylation not affecting *in vitro* activity but increasing *in vitro* protein stability (Huse *et al*, 1988), though no functional phosphosite has so far been identified. Several databases state that yeast

Pfk2 is phosphorylated in Ser652, but they actually refer to a study reporting the phosphorylation of another enzyme, 6-phosphofructo-2-kinase (Pfk26/Yil107c), that catalyses the formation of fructose 2,6-bisphosphate. Our newly identified functional site S163 is located within the initial 200 residues of the N-termimus that are yeast specific (Heinisch *et al*, 1989; Banaszak *et al*, 2011), suggesting that this Pfk2 modification is a yeast specific regulatory mechanism.

For Gpd1, we found that all four phosphosites S23, S24, S25 and S27 are relevant for inhibition of glycerol-3-phosphate dehydrogenase activity. Only the quadruple mutant Gpd1[S23/24/25/27A] showed increased *in vitro* and *in vivo* enzyme activity, displaying a remarkable doubled glycerol yield on glucose relative to the reference strain. Additionally, the relevance of each phosphorylatable serine residue was investigated by targeted phosphoproteomics, revealing that only sites S24 and S27 are phosphorylated in wild-type yeast during growth on glucose and that the protein can occur in both single and double phosphorylated forms (Supplementary Figure 4). However, the double-point mutant Gpd1[S24/27A] did not display altered glycerol yield or enzyme activity (Supplementary Table 3), suggesting that the neigbouring serines S23 and S25 can also be phosphorylated and play a role in the inhibition of Gpd1 activity. The initial, correlation-based indication for phosphorylation activation of Gpd1 was confounded by our inability to differentiate between the Gpd1 and Gpd2 isoenzyme contributions to the flux to glycerol-3-phosphate under the different conditions. Thus, we verified that Gpd1 was the major glycerol-3-phosphate dehydrogenase isoenzyme during growth on glucose (Supplementary Table 3), as was already known for osmotic stress (Blomberg and Adler, 1989; Bouwman *et al*, 2011). Although the yeast response to osmotic stress is known to be mediated through a phosphorylation cascade under the control of the MAP kinase Hog1 (Klipp *et al*, 2005), so far there has not been evidence that Gpd1 activity would be regulated by phosphorylation.

Overall, our study notably expands the current knowledge on the number and role of yeast enzymes that are regulated by post-translational phosphorylation. We provide testable hypotheses for the role of phosphorylation in modulating the functioning of five yeast enzymes not previously known to be functionally phosphoregulated, and verified the impact of phosphorylation for two of them. In particular, we demonstrate the role of phosphorylation in modulating the flux through three central enzymes, which underlines the suspected but presently underappreciated relevance of post-translational modifications in controlling metabolic operation (Heinemann and Sauer, 2010). Thus, the here presented framework that quantitatively relates phosphorylation status with reaction rates opens new opportunities to understand the cellular mechanisms of enzyme regulation by post-translational modifications.

Materials and methods

Detailed descriptions are given in the Supplementary Materials and Methods.

Strains and plasmids

The *S. cerevisiae* strain FY4 *MATa* was used as wild type. Phosphosite mutants were constructed on the related *S. cerevisiae* strain FY3 *MATa ura3-52*. Vector pRS416 was used for cloning. Site-directed mutagenesis was done on plasmids cloned with the native FY4 gene of interest. Plasmids were transformed into FY3 strains in which the corresponding gene locus was deleted from the genome.

Cultivation conditions and physiological characterisation

All cultivations were done aerobically at 30°C in liquid minimum mineral medium supplemented with a carbon source, except otherwise noted. Independent biological triplicates were grown for each condition.

For the five nutritional conditions for phosphoproteomic studies, conditions were the previously used for proteome quantification by SRM (Costenoble *et al*, 2011). Wild-type yeast was grown in shake flasks containing either minimal medium supplemented with 10 g l^{-1} of glucose, galactose or ethanol, anaerobically with 10 g l^{-1} of glucose, or in complex medium containing 20 g l^{-1} yeast extract and 40 g l^{-1} peptone. Samples for phosphoproteomics were harvested in mid-exponential phase at $OD_{600nm} = 1$ (ca. 0.47 g l^{-1} of cell dry weight).

For physiological characterisation of the Pda1 and Gpd1 phosphorylation-deficient mutants, all site mutants and corresponding reference strains were grown in minimal media with 20 g l^{-1} of glucose, in shake flask. Pfk2 phosphorylation-deficient mutants were grown in minimal media with 20 ml l^{-1} of ethanol, also in shake flasks. Samples were taken every half duplication time during the exponential growth phase. Cell density was measured in a spectrophotometer (OD_{600nm}) and the supernant was analysed in a HPLC system for glucose and organic acids concentration. The presence of α-ketoglutarate and glutamine in the Pda1 mutants was confirmed and quantified by LC-MS/MS, according to the method by Buescher *et al* (2010).

For determination of intracellular metabolite concentrations, Pfk2 and Gpd1 mutants and corresponding reference strains were first grown in minimal media with 20 g l^{-1} of glucose, in shake flasks. For Pfk2 mutants, cells were harvested by centrifugation at $OD_{600nm} = 1$, washed and resuspended in the same volume of minimal media with 20 ml l^{-1} of ethanol. Samples for intracellular metabolite quantification were taken 24 h after the shift. For Gpd1 mutants, cells were harvested for intracellular metabolite quantification when the culture reached $OD_{600nm} = 1$.

For determination of *in vitro* glycerol-3-phosphate dehydrogenase activity, Gpd1 mutants and corresponding reference strains were grown in minimal media with 20 g l^{-1} of glucose, in shake flasks, and harvested on ice when the culture reached $OD_{600nm} = 1.5$.

Sample processing for phosphoproteomics

Cell pellets were disrupted by glass beads beating in conditions of protease and phosphatase inhibition. Proteins were precipitated with acetone and digested with trypsin. Peptide mixtures were purified using C18 cartridges (Sep-Pak tC18, Waters), eluted with 60% (v/v) acetonitrile and dried.

For shotgun phosphoproteomics, the peptide mixture was enriched for phosphopeptides by titanium dioxide (TiO_2) chromatography, followed by C18 purification. Dried phosphopeptide mixtures were solubilised in 0.1% formic acid. Related samples were processed in parallel.

MS analysis for phosphoproteomics

For shotgun phosphoproteomic measurements, phosphopeptide mixtures were analysed both on a hybrid LTQ-FT and on a LTQ-Orbitrap mass spectrometer (ThermoFischer Scientific, Bremen, Germany). Samples from galactose-grown cells were analysed only on the LTQ-Orbitrap.

SRM measurements were performed on a TSQ Vantage triple quadruple mass spectrometer (Thermo Fischer Scientific) equipped with a nano-electrospray ion source.

Chromatographic separation was achieved with a nano-LC system (Eksigent) using a linear gradient of ACN/water 0.1% formic acid.

MS spectra processing for phosphoproteomics

For the shotgun MS spectra, the MS2 data were searched against the *S. cerevisiae* SGD non-redundant database using the SORCERER-SEQUEST™ and a target-decoy strategy. Results by Sequest were processed with SuperHirn (v2.0) in a pairwise manner (glucose and one other condition). The SuperHirn output, with the abundance of ion features across replicates, was post-processed as follows: (i) only ion features corresponding to a phosphopeptide with a false discovery rate $<2.5\%$ and at least one phosphorylated serine, threonine and/or tyrosine were selected; (ii) only ion features appearing in all replicates (either in both or only in one condition) were selected; and (iii) peak areas of ion features corresponding to the same phosphopeptide in different charge forms were summed up to one value.

For SRM, traces were manually analysed using the software Skyline. The sum of all transition peak areas monitored for a specific endogenous (light) or standard (heavy) peptide was calculated. From the light versus heavy peptide ratio, we determined relative phosphopeptide changes (for Gpd1 peptides) or absolute endogenous concentrations (for Pda1 and Pfk2 peptides).

SRM data sets associated with this manuscript have been deposited to the PeptideAtlas SRM Experiment Library (PASSEL) and are accessible via the website http://www.peptideatlas.org/passel/. Shotgun data sets have been deposited in the public repository 'PhosphoPep' (http://www.phosphopep.org) and are accessible at http://www.peptideatlas.org/PASS/PASS00037.

Fold-changes in phosphorylation abundance

Fold-changes in phosphopeptide abundance were calculated as the average peak intensity upon growth in each nutrient condition relative to the average peak intensity for glucose-grown samples. When the phosphopeptide was quantified only in the glucose condition or in another condition but not in glucose, the fold-change was considered to be 0.001 or 1000, respectively. For ease of interpretation in Figure 2 and Supplementary Table 2, when the average peak intensity in *ethanol* or *galactose* or *anaerobic* or *complex* (condition 2) was less than in *glucose* (condition 1), the phosphopeptide fold-change was calculated as the negative of the inverse fold-change (for example, -1000 if only detected in glucose), therefore indicating a manyfold higher abundance in the glucose condition. We assume phosphopeptide and phosphoprotein fold-change to be equivalent.

Fold-changes in degree of phosphorylation

For enzymes with both quantified phosphopeptides and total protein, the fold-change in degree of phosphorylation was calculated as the ratio of phosphopeptide fold-change by the total protein fold-change (condition 2 divided by condition 1). For ease of interpretation, values <1 were inverted and signed negative, to indicate the fold-increase in glucose condition.

Correlation analysis between flux and (phospho) protein abundances

Pearson correlation coefficient (R) was used to correlate flux with total protein, phosphoprotein and, when available, non-phosphoprotein abundance fold-changes. The statistical significance of the correlation coefficients (P) was tested using t-statistics $= R \times \sqrt{\frac{N-2}{1-R^2}}$, which follows a t-distribution with $(N-2)$ degrees of freedom. Intracellular fluxes were previously quantified by minimising the total sum of the squared values of all fluxes in a genome-scale stoichiometric metabolic network constrained by measured specific consumption and production rates (Costenoble *et al*, 2011). For Pda1, we considered the upper value of the flux variability analysis (Mahadevan and Schilling, 2003) that obeys our physiological constrains, based on knowledge from literature that activity in ethanol is greater than in glucose (Wenzel *et al*, 1993).

Intracellular metabolites concentration for *in vivo* enzyme activity

In all, 1 ml of culture was sampled into 60% cold methanol for fast quenching of metabolism. Metabolite extraction from cell pellets was done with hot ethanol (80°C, for 3 min), dried, resuspended in doubled distilled water and analysed by LC-MS/MS by SRM. Ion peak areas were normalised relative to a C13 internal standard. Intracellular metabolite concentrations were normalised per unit of OD. Measurements were done in at least two independent biological replicates (Supplementary Table 3).

In vitro glycerol-3-phosphate dehydrogenase activity

In all, 40 ml of culture was harvested on ice and washed once with cold HEPES. Cells were washed and disrupted by beads beating. Cell debris were removed by centrifugation and the supernatant was loaded in a size exclusion Zeba column for removal of salts and small molecules, and resuspended in assay buffer (20 mM imidazole pH 6.5; 0.6 mM $MgCl_2$; 1 mM DTT; complete EDTA-free protease inhibitor cocktail from Roche). Glycerol-3-phosphate dehydrogenase activity was assayed based on the decreased of NADH absorbance at 340 nm (Blomberg and Adler, 1989). The assay was performed in 96-well microtiter plates (Nunc), in a total volume of 200 µl per well (final concentrations: 20 mM imidazole pH 6.5; 0.6 mM $MgCl_2$; 0.15 mM of NADH; and 0.8 mM of dihydroxyacetone phosphate (DHAP; starting reagent)). Enzyme activity was calculated from the linear decrease of absorption over time and expressed in Units per gram of total protein, 1 Unit being 1 µmol of substrate (NADH; extinction coefficient $= 6220\,M^{-1}\,cm^{-1}$; path length of liquid in well $= 0.6$ cm) oxidised per minute. All enzymatic assays were performed at two different dilutions and in biological duplicates.

Supplementary information

Supplementary information is available at the *Molecular Systems Biology* website (www.nature.com/msb).

Acknowledgements

We are thankful to Dr Roeland Costenoble for initial experiments and Dr Bernd Bodenmiller for assistance with shotgun phosphoproteomics measurements. We further thank Dr Mariette Matondo and Dr Nathalie Selevsek for technical assistance with the TSQ instrument, and Stefan Jol, Dr Ludovic Gillet and Stefania Vaga for helpful discussions. This work was funded through the SystemsX.ch project YeastX.

Author contributions: APO, CL, PP, RA and US conceived and designed the study. APO, CL and PP performed the experiments and analysed the results. APO constructed and characterised the mutants, measured the metabolite concentrations, and devised and executed the integrated data analysis. CL developed the SRM assays for quantification of (phospho)peptides, processed the samples and analysed the SRM data. PP measured the phosphoproteome by shotgun. MK helped with the statistics of the data analysis. APO, CL and US wrote the manuscript. All authors read and approved the final manuscript.

Conflict of interest

The authors declare that they have no conflict of interest.

References

Ansell R, Granath K, Hohmann S, Thevelein JM, Adler L (1997) The two isoenzymes for yeast NAD + -dependent glycerol 3-phosphate dehydrogenase encoded by GPD1 and GPD2 have distinct roles in osmoadaptation and redox regulation. *EMBO J* **16:** 2179–2187

Banaszak K, Mechin I, Obmolova G, Oldham M, Chang SH, Ruiz T, Radermacher M, Kopperschlager G, Rypniewski W (2011) The crystal structures of eukaryotic phosphofructokinases from baker's yeast and rabbit skeletal muscle. *J Mol Biol* **407:** 284–297

Blomberg A, Adler L (1989) Roles of glycerol and glycerol-3-phosphate dehydrogenase (NAD+) in acquired osmotolerance of Saccharomyces cerevisiae. *J Bacteriol* **171:** 1087–1092

Bodenmiller B, Aebersold R (2010) Quantitative analysis of protein phosphorylation on a system-wide scale by mass spectrometry-based proteomics. *Methods Enzymol* **470:** 317–334

Bodenmiller B, Campbell D, Gerrits B, Lam H, Jovanovic M, Picotti P, Schlapbach R, Aebersold R (2008) PhosphoPep–a database of protein phosphorylation sites in model organisms. *Nat Biotechnol* **26:** 1339–1340

Bodenmiller B, Wanka S, Kraft C, Urban J, Campbell D, Pedrioli PG, Gerrits B, Picotti P, Lam H, Vitek O, Brusniak MY, Roschitzki B, Zhang C, Shokat KM, Schlapbach R, Colman-Lerner A, Nolan GP, Nesvizhskii AI, Peter M, Loewith R *et al* (2010) Phosphoproteomic analysis reveals interconnected system-wide responses to perturbations of kinases and phosphatases in yeast. *Sci Signal* **3:** rs4

Bouwman J, Kiewiet J, Lindenbergh A, van Eunen K, Siderius M, Bakker BM (2011) Metabolic regulation rather than *de novo* enzyme synthesis dominates the osmo-adaptation of yeast. *Yeast* **28:** 43–53

Breitkreutz A, Choi H, Sharom JR, Boucher L, Neduva V, Larsen B, Lin ZY, Breitkreutz BJ, Stark C, Liu G, Ahn J, Dewar-Darch D, Reguly T, Tang X, Almeida R, Qin ZS, Pawson T, Gingras AC, Nesvizhskii AI, Tyers M (2010) A global protein kinase and phosphatase interaction network in yeast. *Science* **328:** 1043–1046

Buescher JM, Moco S, Sauer U, Zamboni N (2010) Ultrahigh performance liquid chromatography-tandem mass spectrometry method for fast and robust quantification of anionic and aromatic metabolites. *Anal Chem* **82:** 4403–4412

Cohen P (2000) The regulation of protein function by multisite phosphorylation–a 25 year update. *Trends Biochem Sci* **25:** 596–601

Costenoble R, Picotti P, Reiter L, Stallmach R, Heinemann M, Sauer U, Aebersold R (2011) Comprehensive quantitative analysis of central carbon and amino-acid metabolism in Saccharomyces cerevisiae under multiple conditions by targeted proteomics. *Mol Syst Biol* **7:** 464

Daran-Lapujade P, Jansen ML, Daran JM, van Gulik W, de Winde JH, Pronk JT (2004) Role of transcriptional regulation in controlling fluxes in central carbon metabolism of Saccharomyces cerevisiae. A chemostat culture study. *J Biol Chem* **279:** 9125–9138

Daran-Lapujade P, Rossell S, van Gulik WM, Luttik MA, de Groot MJ, Slijper M, Heck AJ, Daran JM, de Winde JH, Westerhoff HV, Pronk JT, Bakker BM (2007) The fluxes through glycolytic enzymes in Saccharomyces cerevisiae are predominantly regulated at posttranscriptional levels. *Proc Natl Acad Sci USA* **104:** 15753–15758

de Godoy LM, Olsen JV, Cox J, Nielsen ML, Hubner NC, Frohlich F, Walther TC, Mann M (2008) Comprehensive mass-spectrometry-based proteome quantification of haploid versus diploid yeast. *Nature* **455:** 1251–1254

Fendt SM, Oliveira AP, Christen S, Picotti P, Dechant RC, Sauer U (2010) Unraveling condition-dependent networks of transcription factors that control metabolic pathway activity in yeast. *Mol Syst Biol* **6:** 432

Fernandez M, Cao J, Vega FV, Hellman U, Wernstedt C, Villamarin JA (1997) cAMP-dependent phosphorylation activates phospho-fructokinase from mantle tissue of the mollusc Mytilus galloprovincialis. Identification of the phosphorylated site. *Biochem Mol Biol Int* **43:** 173–181

Gancedo JM (1998) Yeast carbon catabolite repression. *Microbiol Mol Biol Rev* **62:** 334–361

Gerosa L, Sauer U (2011) Regulation and control of metabolic fluxes in microbes. *Curr Opin Biotechnol* **22:** 566–575

Gey U, Czupalla C, Hoflack B, Rodel G, Krause-Buchholz U (2008) Yeast pyruvate dehydrogenase complex is regulated by a concerted activity of two kinases and two phosphatases. *J Biol Chem* **283:** 9759–9767

Heinemann M, Sauer U (2010) Systems biology of microbial metabolism. *Curr Opin Microbiol* **13:** 337–343

Heinisch J, Ritzel RG, von Borstel RC, Aguilera A, Rodicio R, Zimmermann FK (1989) The phosphofructokinase genes of yeast evolved from two duplication events. *Gene* **78:** 309–321

Holzer H, Purwin C (1986) How does glucose initiate proteolysis of yeast fructose-1,6-bisphosphatase? *Biomed Biochim Acta* **45:** 1657–1663

Huber A, Bodenmiller B, Uotila A, Stahl M, Wanka S, Gerrits B, Aebersold R, Loewith R (2009) Characterization of the rapamycin-sensitive phosphoproteome reveals that Sch9 is a central coordinator of protein synthesis. *Genes Dev* **23:** 1929–1943

Huse K, Jergil B, Schwidop WD, Kopperschlager G (1988) Evidence for phosphorylation of yeast phosphofructokinase. *FEBS Lett* **234:** 185–188

Huttlin EL, Jedrychowski MP, Elias JE, Goswami T, Rad R, Beausoleil SA, Villen J, Haas W, Sowa ME, Gygi SP (2010) A tissue-specific atlas of mouse protein phosphorylation and expression. *Cell* **143:** 1174–1189

Kemp RG, Foe LG (1983) Allosteric regulatory properties of muscle phosphofructokinase. *Mol Cell Biochem* **57:** 147–154

Klipp E, Nordlander B, Kruger R, Gennemark P, Hohmann S (2005) Integrative model of the response of yeast to osmotic shock. *Nat Biotechnol* **23:** 975–982

Krause-Buchholz U, Gey U, Wunschmann J, Becker S, Rodel G (2006) YIL042c and YOR090c encode the kinase and phosphatase of the Saccharomyces cerevisiae pyruvate dehydrogenase complex. *FEBS Lett* **580:** 2553–2560

Krebs EG, Beavo JA (1979) Phosphorylation-dephosphorylation of enzymes. *Annu Rev Biochem* **48:** 923–959

Landry CR, Levy ED, Michnick SW (2009) Weak functional constraints on phosphoproteomes. *Trends Genet* **25:** 193–197

Larsen MR, Thingholm TE, Jensen ON, Roepstorff P, Jorgensen TJ (2005) Highly selective enrichment of phosphorylated peptides from peptide mixtures using titanium dioxide microcolumns. *Mol Cell Proteomics* **4:** 873–886

Legisa M, Bencina M (1994) Evidence for the activation of 6-phosphofructo-1-kinase by cAMP-dependent protein kinase in Aspergillus niger. *FEMS Microbiol Lett* **118:** 327–333

Lin K, Rath VL, Dai SC, Fletterick RJ, Hwang PK (1996) A protein phosphorylation switch at the conserved allosteric site in GP. *Science* **273:** 1539–1542

Mahadevan R, Schilling CH (2003) The effects of alternate optimal solutions in constraint-based genome-scale metabolic models. *Metab Eng* **5:** 264–276

Oliveira AP, Sauer U (2012) The importance of post-translational modifications in regulating Saccharomyces cerevisiae metabolism. *FEMS Yeast Res* **12:** 104–117

Olsen JV, Vermeulen M, Santamaria A, Kumar C, Miller ML, Jensen LJ, Gnad F, Cox J, Jensen TS, Nigg EA, Brunak S, Mann M (2010) Quantitative phosphoproteomics reveals widespread full phosphorylation site occupancy during mitosis. *Sci Signal* **3:** ra3

Picotti P, Bodenmiller B, Mueller LN, Domon B, Aebersold R (2009) Full dynamic range proteome analysis of S. cerevisiae by targeted proteomics. *Cell* **138:** 795–806

Ptacek J, Devgan G, Michaud G, Zhu H, Zhu X, Fasolo J, Guo H, Jona G, Breitkreutz A, Sopko R, McCartney RR, Schmidt MC, Rachidi N, Lee SJ, Mah AS, Meng L, Stark MJ, Stern DF, De Virgilio C, Tyers M *et al* (2005) Global analysis of protein phosphorylation in yeast. *Nature* **438:** 679–684

San Miguel PF, Arguelles JC (1994) Differential changes in the activity of cytosolic and vacuolar trehalases along the growth cycle of Saccharomyces cerevisiae. *Biochim Biophys Acta* **1200:** 155–160

Sauer U (2006) Metabolic networks in motion: 13C-based flux analysis. *Mol Syst Biol* **2:** 62

Serber Z, Ferrell Jr JE (2007) Tuning bulk electrostatics to regulate protein function. *Cell* **128:** 441–444

Smith TL, Rutter J (2007) Regulation of glucose partitioning by PAS kinase and Ugp1 phosphorylation. *Mol Cell* **26:** 491–499

Tyson JJ, Novak B (2008) Temporal organization of the cell cycle. *Curr Biol* **18:** R759–R768

Uhlinger DJ, Yang CY, Reed LJ (1986) Phosphorylation-dephosphorylation of pyruvate dehydrogenase from bakers' yeast. *Biochemistry* **25:** 5673–5677

Wenzel TJ, Luttik MA, van den Berg JA, de Steensma HY (1993) Regulation of the PDA1 gene encoding the E1 alpha subunit of the pyruvate dehydrogenase complex from Saccharomyces cerevisiae. *Eur J Biochem* **218:** 405–411

Wera S, De Schrijver E, Geyskens I, Nwaka S, Thevelein JM (1999) Opposite roles of trehalase activity in heat-shock recovery and heat-shock survival in Saccharomyces cerevisiae. *Biochem J* **343**(Part 3)**:** 621–626

Westergaard SL, Oliveira AP, Bro C, Olsson L, Nielsen J (2007) A systems biology approach to study glucose repression in the yeast Saccharomyces cerevisiae. *Biotechnol Bioeng* **96:** 134–145

Wu R, Dephoure N, Haas W, Huttlin EL, Zhai B, Sowa ME, Gygi SP (2011a) Correct interpretation of comprehensive phosphorylation dynamics requires normalization by protein expression changes. *Mol Cell Proteomics* **10**(M111)**:** 009654

Wu R, Haas W, Dephoure N, Huttlin EL, Zhai B, Sowa ME, Gygi SP (2011b) A large-scale method to measure absolute protein phosphorylation stoichiometries. *Nat Methods* **8:** 677–683

Wu YB, Dai J, Yang XL, Li SJ, Zhao SL, Sheng QH, Tang JS, Zheng GY, Li YX, Wu JR, Zeng R (2009) Concurrent quantification of proteome and phosphoproteome to reveal system-wide association of protein phosphorylation and gene expression. *Mol Cell Proteomics* **8:** 2809–2826

Xu YF, Zhao X, Glass DS, Absalan F, Perlman DH, Broach JR, Rabinowitz JD (2012) Regulation of yeast pyruvate kinase by ultrasensitive allostery independent of phosphorylation. *Mol Cell* **48**(1)**:** 52–62